of up to ~1500 Å^3. Structures in which as many as 70 parameters were refined have been successfully determined with use of steady-state reactor sources and the Rietveld technique.[13]

The 0.2–0.3% resolution of the intense pulsed neutron source (IPNS-I) general purpose powder diffractometer, and the projected IPNS-I flux, should allow an entire powder spectrum to be collected in less than 1 day. Thus the use of polycrystalline samples, rather than large single crystals, opens the field of neutron diffraction to a large number of chemical problems not previously accessible.[16]

Acknowledgment. J.M.W. wishes to thank NATO (Research Grant No. 1276) for support which made it possible to visit and exchange information with European scientists. We wish to thank Professor W. A. Freeman, who assisted in early X-ray studies.

Registry No. $Tl_4[Pt(CN)_4]CO_3$, 76880-00-7.

Supplementary Material Available: A listing of structure factor amplitudes (1 page). Ordering information is given on any current masthead page.

---

(13) Cheetham, A. K.; Taylor, J. C. *J. Solid State Chem.* **1977**, *21*, 253.

(14) Jorgensen, J. D.; Rotella, F. J. *J. Appl. Crytallogr.*, in press. See also: Lager, G. A.; Ross, F. K.; Rotella, F. J.; Jorgensen, J. D. *Ibid.* **1981**, *14*, 137.

(15) For a discussion, see: Prince, E. *J. Appl. Crystallogr.*, in press.

(16) ZING-P′ is the prototype of a new pulsed neutron source IPNS-I which will start operating in the spring of 1981. IPNS-I will be a national user facility for condensed matter research, available to all qualified scientists according to policies established by the Department of Energy. Inquiries should be addressed to Dr. T. G. Worlton, Scientific Secretary, IPNS Program, Argonne National Laboratory, Argonne, IL 60439.

Contribution from the Departments of Chemistry, Brookhaven National Laboratory, Upton, New York 11973,
and University of California, Berkeley, California 94720, and the Chemistry Division,
Argonne National Laboratory, Argonne, Illinois 60439

Crystal Structure of $\{HRh[P(O\text{-}i\text{-}C_3H_7)_3]_2\}_2$. A Neutron Diffraction Study

R. G. TELLER,[1a] JACK M. WILLIAMS,*[1a] T. F. KOETZLE,[1b] R. R. BURCH,[1c] R. M. GAVIN,[1d]
and E. L. MUETTERTIES*[1c]

Received August 1, 1980

A neutron diffraction study of $\{HRh[P(O\text{-}i\text{-}C_3H_7)_3]_2\}_2$ confirmed the square-planar coordination geometry inferred from spectroscopic data and accurately placed the hydride ligands at bridging positions. At 112.4 K, the crystal lattice was triclinic, of space group $P\bar{1}$, with a = 12.084 (3) Å, b = 13.505 (6) Å, c = 9.540 (2) Å, α = 97.49 (2)°, β = 105.18 (1)°, γ = 116.15 (2)°, V_c = 1074.4 Å^3, and Z = 1. The Rh–Rh distances were 2.65 (1) Å, and the Rh–H distances were 1.808 (14) Å with H–Rh–H and Rh–H–Rh angles of 85.9 (5) and 94.1 (4)°, respectively. With an only slightly expanded P–Rh–P angle of 94.7 (4)°, near 90° average H–Rh–P angles, and near coplanarity of the $H_2Rh_2P_4$ system, the square-planar coordination geometry about each rhodium atom was established unequivocally. The planar Rh_2H_2 system is rectangular with 2.65- and 2.46-Å diagonals. Two four-center (Rh_2H_2) two-electron bonds are responsible for the framework bonding in the dimer. The net Mulliken bond order for the direct Rh–Rh interaction is positive but very small whereas those for Rh–H are large, nearly 0.5, as indicated by a molecular orbital analysis.

Introduction

Chemical studies[2] of $\{HRh[P(O\text{-}i\text{-}C_3H_7)_3]_2\}_2$ have been providing molecular and mechanistic insights to catalytic reactions that involve both metal atoms of a coordinately unsaturated dinuclear metal complex. Because of the chemical importance of this molecule and the related $\{HRh[P(OCH_3)_3]_2\}_3$ complex, a neutron structure determination was undertaken, and the crystallographic[3] results are reported here.

Experimental Section

Crystals of $\{HRh[P(O\text{-}i\text{-}C_3H_7)_3]_2\}_2$ were obtained by slow cooling of pentane solutions of the dimeric hydride. A rectangular crystal with faces with indices of the forms [02$\bar{3}$], [$\bar{3}$10], and [010] and with a volume of ~17 mm^3 was used for data collection. The crystal was mounted in a glass capillary, and the capillary was affixed to a hollow aluminum pin. This pin was mounted in an aluminum housing in a helium atmosphere, and this sample holder was placed in a closed-cycle helium refrigerator. During the course of preliminary crystallographic investigations and data collection the crystal was maintained at 112.4 K. Neutron diffraction data were collected[4] at the Brookhaven National Laboratory high flux beam reactor. The neutron beam wavelength was 1.1617 (1) Å. This wavelength was determined prior to the experiment by a least-squares fit of 48 reflections using a KBr crystal (a = 6.6000 Å). For minimization of the scattering from the refrigerator walls, a 12 in. Masonite collimator with a LiF extender (i.d. $^5/_8$ in.) was utilized.

Table I. Details of Data Collection and Structure Refinement for $\{HRh[P(O\text{-}i\text{-}C_3H_7)_3]_2\}_2$

cryst system	triclinic, $P\bar{1}$, Z = 1
cell const (112.4 K)	
a, Å	12.084 (3)
b, Å	13.505 (6)
c, Å	9.540 (2)
α, deg	97.49 (2)
β, deg	105.18 (1)
γ, deg	116.15 (2)
V_c, Å^3	1074.4
mol wt	1040.8
D(calcd), g/cm^3	1.61
abs coeff, cm^{-1}	3.39
min and max transmission factors	0.521–0.730
data collection limit, Å^{-1} ((sin θ)/λ)	0.581 Å^{-1} (4224 reflections)
final agreement factor[a]	$R_w(F_o^2)$ = 0.135 (0.119)
goodness of fit	2.13
observn to parameter ratio	6.25

[a] Number in parentheses refers to data with $F_o^2 > \sigma(F_o^2)$.

Despite its adequate size, the crystal was a poor scatterer. The average peak full width at half-height was 0.45° in ω; difficulty was encountered in finding intense reflections to center for accurate lattice constant determination. Additionally, a significant (sin θ)/λ falloff in intensities was noted at 112.4 K. However, because of the chemical importance of the dimer and the lack of more suitable crystals, it was

---

(1) (a) Argonne National Laboratory. (b) Brookhaven National Laboratory. (c) University of California. (d) Department of Chemistry, Haverford College, Haverford, PA.

(2) (a) V. W. Day, M. F. Friedrich, G. S. Reddy, A. J. Sivak, W. R. Pretzer, and E. L. Muetterties, *J. Am. Chem. Soc.*, **99**, 8091 (1977); (b) A. J. Sivak and E. L. Muetterties, *ibid.*, **101**, 4878 (1979).

(3) R. K. Brown, J. M. Williams, M. F. Friedrich, V. W. Day, A. J. Sivak, and E. L. Muetterties, *Proc. Natl. Acad. Sci. U.S.A.*, **76**, 2099 (1979).

(4) (a) D. G. Dimmler, N. Greenlaw, M. A. Kelley, D. W. Potter, S. Rankowitz, and F. W. Stubblefied, *IEEE Trans. Nucl. Sci.*, **23**, 398 (1976); (b) R. K. McMullan, L. C. Andrews, T. F. Koetzle, F. Reidinger, R. Thomas, and G. J. B. Williams, NEXDAS Neutron and X-Ray Data Acquisition System, unpublished results.

0020-1669/81/1320-1806$01.25/0

Table II. Final Positional[a] and Thermal[b] Parameters for $\{HRh[P(O\text{-}i\text{-}C_3H_7)_3]_2\}_2$

atom	x	y	z	U_{11}	U_{22}	U_{33}	U_{12}	U_{13}	U_{23}
Rh	0.0297 (5)	0.1084 (5)	0.0459 (6)	0.010 (3)	0.047 (4)	0.017 (3)	0.011 (3)	−0.000 (2)	−0.004 (3)
H	0.108 (1)	0.024 (1)	0.090 (2)	0.020 (5)	0.07 (1)	0.11 (1)	0.02 (1)	0.01 (1)	−0.01 (1)
P(1)	−0.0735 (6)	0.2032 (6)	−0.0090 (7)	0.035 (4)	0.035 (4)	0.015 (4)	0.011 (3)	0.002 (3)	−0.006 (3)
P(2)	0.2057 (6)	0.2551 (6)	0.2161 (9)	0.031 (4)	0.035 (5)	0.046 (5)	0.016 (3)	−0.010 (4)	−0.002 (4)
O(11)	−0.2120 (5)	0.1226 (6)	−0.1448 (8)	0.018 (3)	0.060 (5)	0.039 (5)	0.013 (3)	0.002 (3)	0.003 (4)
O(12)	−0.1119 (8)	0.2615 (8)	0.1135 (8)	0.08 (1)	0.09 (1)	0.037 (5)	0.07 (1)	0.008 (4)	0.04 (1)
O(13)	−0.010 (1)	0.315 (1)	−0.072 (1)	0.06 (1)	0.11 (1)	0.12 (1)	0.03 (1)	0.02 (1)	0.10 (1)
O(21)	0.3383 (7)	0.2933 (8)	0.187 (2)	0.017 (4)	0.07 (1)	0.28 (2)	0.011 (4)	−0.00 (1)	−0.06 (1)
O(22)	0.243 (2)	0.231 (1)	0.379 (1)	0.27 (2)	0.04 (1)	0.06 (1)	0.03 (1)	−0.07 (1)	−0.01 (1)
O(23)	0.2082 (6)	0.3705 (6)	0.2693 (7)	0.032 (4)	0.050 (5)	0.026 (4)	0.014 (3)	−0.001 (3)	0.015 (4)
C(11A)	−0.3037 (6)	0.1625 (6)	−0.2098 (8)	0.049 (4)	0.064 (5)	0.046 (5)	0.021 (4)	−0.017 (3)	0.007 (4)
C(11B)	−0.436 (1)	0.089 (1)	−0.196 (1)	0.061 (6)	0.215 (13)	0.113 (9)	0.088 (7)	0.055 (6)	0.117 (9)
C(11C)	−0.320 (1)	0.172 (1)	−0.358 (1)	0.07 (1)	0.14 (1)	0.07 (1)	0.02 (1)	0.02 (1)	0.04 (1)
C(12A)	−0.1066 (6)	0.2354 (6)	0.2513 (7)	0.049 (4)	0.072 (5)	0.043 (4)	0.042 (4)	0.005 (3)	0.015 (4)
C(12B)	−0.220 (1)	0.119 (1)	0.221 (1)	0.08 (1)	0.11 (1)	0.08 (1)	0.05 (1)	0.03 (1)	0.04 (1)
C(12C)	−0.126 (1)	0.323 (1)	0.345 (1)	0.18 (1)	0.19 (1)	0.04 (1)	0.17 (1)	0.03 (1)	0.03 (1)
C(13A)	0.0934 (7)	0.3658 (8)	−0.102 (1)	0.038 (4)	0.12 (1)	0.15 (1)	−0.006 (5)	0.00 (1)	0.11 (1)
C(13B)	0.051 (1)	0.275 (2)	−0.261 (2)	0.08 (1)	0.57 (4)	0.12 (1)	0.04 (2)	0.03 (1)	0.19 (2)
C(13C)	0.160 (1)	0.472 (1)	−0.112 (3)	0.10 (1)	0.13 (1)	0.33 (3)	−0.04 (1)	0.03 (1)	0.14 (1)
C(21A)	0.3588 (7)	0.2416 (7)	0.067 (1)	0.048 (5)	0.08 (1)	0.13 (1)	0.018 (5)	0.06 (1)	0.03 (1)
C(21B)	0.428 (1)	0.178 (1)	0.129 (1)	0.05 (1)	0.10 (1)	0.15 (1)	0.05 (1)	0.03 (1)	−0.01 (1)
C(21C)	0.453 (1)	0.349 (1)	0.057 (2)	0.07 (1)	0.20 (2)	0.32 (2)	0.07 (1)	0.08 (1)	0.17 (2)
C(22A)	0.2034 (6)	0.1380 (8)	0.431 (1)	0.028 (3)	0.09 (1)	0.08 (1)	0.022 (4)	0.019 (4)	0.06 (1)
C(22B)	0.282 (1)	0.112 (1)	0.509 (2)	0.07 (1)	0.23 (1)	0.29 (2)	0.09 (1)	0.04 (1)	0.20 (1)
C(22C)	0.062 (1)	0.042 (1)	0.400 (2)	0.04 (1)	0.03 (1)	0.06 (1)	0.02 (1)	0.03 (1)	0.03 (1)
C(22C′)	0.227 (2)	0.229 (1)	0.568 (2)	0.13 (2)	0.03 (1)	0.04 (1)	0.01 (1)	0.03 (1)	0.02 (1)
C(23A)	0.3227 (7)	0.4728 (5)	0.3886 (9)	0.055 (4)	0.028 (4)	0.07 (1)	0.017 (4)	−0.001 (4)	−0.002 (4)
C(23B)	0.285 (1)	0.512 (1)	0.489 (2)	0.17 (1)	0.12 (1)	0.13 (1)	0.02 (1)	0.08 (1)	−0.04 (1)
C(23C)	0.402 (1)	0.561 (1)	0.353 (2)	0.10 (1)	0.11 (1)	0.21 (2)	0.03 (1)	0.06 (1)	0.09 (1)
H(11A)	−0.264 (2)	0.251 (1)	−0.139 (2)	0.11 (1)	0.04 (1)	0.17 (2)	0.04 (1)	−0.09 (1)	−0.04 (1)
H(11B1)	−0.417 (2)	0.103 (3)	−0.074 (2)	0.21 (2)	0.62 (6)	0.09 (1)	0.33 (4)	0.10 (2)	0.15 (2)
H(11B2)	−0.501 (1)	0.110 (2)	−0.237 (2)	0.07 (1)	0.20 (2)	0.07 (1)	0.09 (1)	0.04 (1)	0.07 (1)
H(11B3)	−0.471 (1)	0.003 (1)	−0.266 (3)	0.05 (1)	0.07 (1)	0.18 (2)	−0.01 (1)	0.02 (1)	0.02 (1)
H(11C1)	−0.371 (3)	0.076 (4)	−0.446 (2)	0.27 (4)	0.54 (7)	−0.00 (1)	0.17 (4)	−0.00 (1)	−0.04 (2)
H(11C2)	−0.229 (2)	0.195 (3)	−0.383 (2)	0.09 (1)	0.41 (4)	0.12 (2)	0.07 (2)	0.05 (1)	0.17 (2)
H(11C3)	−0.371 (1)	0.192 (2)	−0.392 (2)	0.07 (1)	0.13 (2)	0.12 (2)	0.04 (1)	0.06 (1)	0.05 (1)
H(12A)	−0.021 (1)	0.235 (1)	0.306 (1)	0.08 (1)	0.16 (2)	0.04 (1)	0.08 (1)	0.03 (1)	0.04 (1)
H(12B1)	−0.232 (2)	0.099 (1)	0.318 (2)	0.13 (1)	0.09 (1)	0.18 (2)	0.06 (1)	0.11 (1)	0.09 (1)
H(12B2)	−0.208 (2)	0.057 (2)	0.149 (3)	0.13 (2)	0.18 (2)	0.22 (3)	0.07 (2)	0.14 (2)	0.11 (2)
H(12B3)	−0.324 (2)	0.114 (3)	0.163 (3)	0.05 (1)	0.49 (6)	0.20 (3)	0.07 (2)	0.03 (1)	0.21 (4)
H(12C1)	−0.213 (2)	0.324 (2)	0.294 (2)	0.17 (2)	0.31 (3)	0.11 (2)	0.21 (2)	0.06 (1)	0.07 (2)
H(12C2)	−0.114 (2)	0.320 (2)	0.452 (2)	0.10 (1)	0.10 (1)	0.13 (2)	0.03 (1)	0.06 (1)	0.01 (1)
H(12C3)	−0.037 (3)	0.414 (2)	0.355 (3)	0.27 (3)	0.07 (1)	0.15 (2)	0.12 (2)	0.10 (2)	0.02 (1)
H(13A)	0.172 (1)	0.348 (2)	−0.029 (2)	0.07 (1)	0.17 (2)	0.12 (2)	0.04 (1)	−0.01 (1)	0.08 (1)
H(13B1)	−0.024 (3)	0.285 (6)	−0.330 (4)	0.12 (2)	1.2 (2)	0.22 (4)	0.10 (5)	0.05 (2)	0.45 (7)
H(13B2)	0.029 (2)	0.200 (2)	−0.264 (2)	0.12 (2)	0.21 (2)	0.09 (2)	−0.00 (2)	0.06 (1)	0.05 (2)
H(13B3)	0.117 (6)	0.299 (7)	−0.313 (5)	0.51 (8)	0.8 (1)	0.15 (4)	−0.05 (8)	0.24 (5)	0.15 (6)
H(13C1)	0.205 (3)	0.518 (2)	−0.061 (3)	0.29 (4)	0.14 (2)	0.13 (2)	0.10 (3)	0.14 (2)	0.04 (2)
H(13C2)	0.090 (4)	0.539 (2)	−0.065 (5)	0.51 (6)	0.14 (3)	0.57 (7)	0.16 (3)	0.45 (5)	0.20 (4)
H(13C3)	0.199 (2)	0.461 (2)	−0.196 (3)	0.23 (3)	0.26 (3)	0.27 (3)	0.13 (2)	0.22 (3)	0.20 (3)
H(21A)	0.270 (2)	0.189 (2)	−0.021 (2)	0.08 (1)	0.17 (2)	0.16 (2)	0.08 (1)	0.05 (1)	0.08 (2)
H(21B1)	0.513 (1)	0.232 (1)	0.215 (2)	0.06 (1)	0.12 (1)	0.14 (2)	0.06 (1)	0.04 (1)	0.04 (1)
H(21B2)	0.360 (1)	0.103 (1)	0.173 (2)	0.07 (1)	0.07 (1)	0.19 (2)	0.02 (1)	0.03 (1)	0.02 (1)
H(21B3)	0.441 (1)	0.141 (2)	0.027 (3)	0.04 (1)	0.13 (2)	0.20 (2)	−0.01 (1)	0.02 (1)	−0.10 (2)
H(21C1)	0.525 (3)	0.396 (2)	0.118 (4)	0.10 (2)	0.11 (2)	0.40 (5)	0.01 (2)	−0.02 (3)	0.00 (3)
H(21C2)	0.394 (4)	0.384 (3)	−0.019 (4)	0.35 (6)	0.29 (4)	0.34 (4)	0.18 (4)	−0.12 (4)	0.13 (4)
H(21C3)	0.490 (5)	0.313 (6)	−0.042 (9)	0.23 (5)	0.7 (1)	1.0 (1)	0.28 (6)	0.37 (7)	0.7 (1)
H(22A)	0.248 (6)	0.216 (7)	0.528 (5)	0.26 (6)	0.28 (9)	0.09 (4)	0.20 (7)	0.08 (4)	0.12 (5)
H(22A′)	0.126 (5)	0.103 (2)	0.348 (3)	0.28 (6)	0.03 (2)	0.03 (2)	−0.07 (3)	0.02 (3)	−0.00 (2)
H(22B1)	0.236 (3)	0.045 (2)	0.543 (3)	0.26 (3)	0.21 (3)	0.27 (3)	0.20 (3)	0.19 (3)	0.19 (3)
H(22B2)	0.377 (3)	0.174 (4)	0.575 (4)	0.15 (3)	0.54 (7)	0.20 (4)	0.19 (4)	−0.08 (3)	0.04 (4)
H(22B3)	0.273 (5)	0.071 (3)	0.374 (6)	0.61 (9)	0.24 (4)	0.6 (1)	0.26 (5)	0.59 (9)	0.27 (6)
H(22C1)	−0.015 (3)	0.010 (3)	0.280 (4)	0.08 (2)	0.10 (2)	0.12 (3)	0.07 (2)	0.05 (2)	0.08 (2)
H(22C1′)	0.307 (5)	0.302 (3)	0.659 (4)	0.26 (5)	0.07 (2)	0.03 (2)	0.00 (3)	0.05 (3)	−0.04 (2)
H(22C2)	0.035 (3)	0.079 (3)	0.479 (3)	0.10 (2)	0.08 (2)	0.05 (2)	0.06 (2)	0.03 (2)	0.04 (2)
H(22C2′)	0.216 (6)	0.184 (3)	0.662 (3)	0.4 (1)	0.05 (2)	0.02 (2)	0.02 (4)	0.11 (3)	0.03 (2)
H(22C3)	0.058 (8)	−0.039 (3)	0.45	0.4 (1)	0.04 (3)	0.9 (2)	0.15 (5)	−0.3 (1)	−0.1 (1)
H(22C3′)	0.159 (5)	0.267 (7)	0.56	0.07 (4)	0.3 (1)	1.0 (2)	0.13 (6)	−0.06 (8)	0.1 (1)
H(23A)	0.398 (1)	0.458 (1)	0.429 (2)	0.06 (1)	0.08 (1)	0.16 (2)	0.03 (1)	−0.09 (1)	−0.08 (1)
H(23B1)	0.225 (3)	0.441 (2)	0.527 (2)	0.32 (4)	0.16 (3)	0.08 (2)	−0.02 (2)	0.09 (2)	−0.01 (2)
H(23B2)	0.215 (3)	0.550 (2)	0.415 (2)	0.30 (3)	0.12 (2)	0.11 (2)	0.12 (2)	0.11 (2)	0.06 (1)
H(23B3)	0.353 (2)	0.582 (2)	0.590 (3)	0.16 (2)	0.18 (3)	0.11 (2)	−0.05 (2)	−0.04 (2)	−0.10 (2)
H(23C1)	0.310 (5)	0.586 (3)	0.233 (4)	0.6 (1)	0.16 (3)	0.23 (4)	0.20 (4)	0.23 (5)	0.15 (3)
H(23C2)	0.452 (3)	0.536 (4)	0.298 (5)	0.19 (4)	0.48 (7)	0.66 (8)	0.27 (5)	0.25 (5)	0.45 (6)
H(23C3)	0.4511 (2)	0.622 (2)	0.430 (2)	0.11 (1)	0.10 (2)	0.19 (2)	0.07 (1)	0.03 (1)	0.02 (2)

[a] x, y, and z are given in fractional coordinates. [b] Anisotropic temperature factors are of the form $\exp[-2\pi^2(a^{*2}U_{11}h^2 + \ldots + 2a^*b^*U_{12}hk + \ldots)]$.

Table III. Some Distances (A) and Angles (Deg) in $\{HRh[P(O\text{-}i\text{-}C_3H_7)_3]_2\}_2$[a,b]

A. Distances

Rh-H	1.805 (14)	Rh-P(1)	2.170 (9)
Rh-H′	1.812 (13)	Rh-P(2)	2.173 (8)
Rh-Rh′	2.647 (13)	H· · ·H′	2.465 (14)
P(1)-O(11)	1.598 (8)	P(2)-O(21)	1.559 (10)
P(1)-O(12)	1.601 (10)	P(2)-O(22)	1.568 (13)
P(1)-O(13)	1.635 (10)	P(2)-O(23)	1.622 (13)
O(11)-C(11A)	1.47 (1)	O(21)-C(21A)	1.39 (2)
O(12)-C(12A)	1.40 (1)	O(22)-C(22A)	1.34 (1)
O(13)-C(13A)	1.26 (1)	O(23)-C(23A)	1.48 (1)
C(11A)-C(11B)	1.40 (1)	C(21A)-C(21B)	1.51 (1)
C(11A)-C(11C)	1.52 (1)	C(21A)-C(21C)	1.43 (1)
C(12A)-C(12B)	1.49 (1)	C(22A)-C(22B)	1.25 (1)
C(12A)-C(12C)	1.53 (1)	C(22A)-C(22C)	1.54 (1), 1.54 (2)[c]
C(13A)-C(13B)	1.62 (3)	C(23A)-C(23B)	1.31 (1)
C(13A)-C(13C)	1.34 (2)	C(23A)-C(23C)	1.31 (1)
C(11A)-H(11A)	1.11 (2)	C(21A)-H(21A)	1.03 (2)
C(11B)-H(11B1)	1.09 (2)	C(21B)-H(21B1)	1.00 (2)
C(11B)-H(11B2)	0.97 (2)	C(21B)-H(21B2)	1.12 (2)
C(11B)-H(11B3)	1.09 (3)	C(21B)-H(21B3)	1.19 (2)
C(11C)-H(11C1)	1.22 (4)	C(21C)-H(21C1)	0.81 (3)
C(11C)-H(11C2)	1.10 (3)	C(21C)-H(21C2)	1.17 (8)
C(11C)-H(11C3)	0.80 (2)	C(21C)-H(21C3)	1.27 (7)
C(12A)-H(12A)	1.03 (2)	C(22A)-H(22A)	1.11 (7), 0.92 (5)
C(12B)-H(12B1)	1.03 (2)	C(22B)-H(22B1)	0.98 (3)
C(12B)-H(12B2)	1.10 (3)	C(22B)-H(22B2)	1.02 (3)
C(12B)-H(12B3)	1.20 (2)	C(22B)-H(22B3)	1.29 (6)
C(12C)-H(12C1)	1.04 (2)	C(22C)-H(22C1)	1.15 (4), 1.08 (4)
C(12C)-H(12C2)	1.00 (3)	C(22C)-H(22C2)	1.05 (4), 1.14 (4)
C(12C)-H(12C3)	1.20 (3)	C(22C)-H(22C3)	1.24 (7), 1.14 (6)
C(13A)-H(13A)	1.15 (2)	C(23A)-H(23A)	1.01 (2)
C(13B)-H(13B1)	1.04 (5)	C(23B)-H(23B1)	1.09 (4)
C(13B)-H(13B2)	0.92 (3)	C(23B)-H(23B2)	1.27 (4)
C(13B)-H(13B3)	1.01 (4)	C(23B)-H(23B3)	1.07 (2)
C(13C)-H(13C1)	0.65 (3)	C(23C)-H(23C1)	1.55 (6)
C(13C)-H(13C2)	1.56 (5)	C(23C)-H(23C2)	1.02 (4)
C(13C)-H(13C3)	1.05 (3)	C(23C)-H(23C3)	0.88 (3)

B. Angles

H-Rh-H′	85.9 (5)	H-Rh-P(2)	87.5 (4)
H-Rh-P(1)	177.3 (5)	H′-Rh-P(2)	173.4 (5)
H′-Rh-P(1)	91.8 (4)	P(1)-Rh-P(2)	94.7 (4)
Rh-H-Rh′	94.1 (4)	Rh′-Rh-P(1)	134.6 (4)
		Rh′-Rh-P(2)	130.6 (4)
Rh-P(1)-O(11)	110.4 (5)	Rh-P(2)-O(21)	116.6 (5)
Rh-P(1)-O(12)	122.1 (5)	Rh-P(2)-O(22)	112.7 (5)
Rh-P(1)-O(13)	120.3 (5)	Rh-P(2)-O(23)	120.8 (5)
O(11)-P(1)-O(12)	103.2 (5)	O(21)-P(2)-O(22)	101.3 (8)
O(11)-P(1)-O(13)	100.9 (5)	O(21)-P(2)-O(23)	103.9 (6)
O(12)-P(1)-O(13)	96.8 (6)	O(22)-P(2)-O(23)	98.5 (7)
P(1)-O(11)-C(11A)	123.4 (6)	P(2)-O(21)-C(21A)	127.9 (7)
P(1)-O(12)-C(12A)	122.2 (6)	P(2)-O(22)-C(22A)	135.5 (8)
P(1)-O(13)-C(13A)	135.4 (9)	P(2)-O(23)-C(23A)	123.8 (5)
O(11)-C(11A)-C(11B)	109.2 (6)	O(21)-C(21A)-C(21B)	107.0 (9)
O(11)-C(11A)-C(11C)	116.9 (8)	O(21)-C(21A)-C(21C)	93.7 (11)
O(11)-C(11A)-H(11A)	107.2 (8)	O(21)-C(21A)-H(21A)	109.6 (11)
C(11B)-C(11A)-C(11C)	111.3 (6)	C(21B)-C(21A)-C(21C)	109.8 (7)
C(11B)-C(11A)-H(11A)	107.0 (14)	C(21B)-C(21A)-H(21A)	113.3 (12)
C(11C)-C(11A)-H(11A)	104.6 (13)	C(21C)-C(21A)-H(21A)	120.9 (14)
O(12)-C(12A)-C(12B)	108.1 (7)	O(22)-C(22A)-C(22B)	123.2 (9)
O(12)-C(12A)-C(12C)	105.7 (6)	O(22)-C(22A)-C(22C)	129.0 (9), 80.0 (10)
O(12)-C(12A)-H(12A)	113.7 (9)	O(22)-C(22A)-H(22A)	71.4 (28), 87.9 (20)
C(12B)-C(12A)-C(12C)	108.2 (8)	C(22B)-C(22A)-C(22C)	107.6 (8), 92.6 (12)
C(12B)-C(12A)-H(12A)	108.1 (11)	C(22B)-C(22A)-H(22A)	86.5 (26), 139.1 (31)
C(12C)-C(12A)-H(12A)	113.0 (10)	C(22C)-C(22A)-H(22A)	117.9 (29), 120.7 (37)
O(13)-C(13A)-C(13B)	99.2 (9)	O(23)-C(23A)-C(23B)	110.6 (8)
O(13)-C(13A)-C(13C)	132.5 (15)	O(23)-C(23A)-C(23C)	120.8 (9)
O(13)-C(13A)-H(13A)	107.4 (11)	O(23)-C(23A)-H(23A)	111.1 (9)
C(13B)-C(13A)-C(13C)	108.8 (14)	C(23B)-C(23A)-C(23C)	107.7 (10)
C(13B)-C(13A)-H(13A)	98.0 (15)	C(23B)-C(23A)-H(23A)	116.3 (16)
C(13C)-C(13A)-H(13A)	105.7 (12)	C(23C)-C(23A)-H(23A)	89.1 (15)
C(11A)-C(11B)-H(11B1)	105.9 (15)	C(21A)-C(21B)-H(21B1)	110.3 (11)
C(11A)-C(11B)-H(11B2)	113.0 (11)	C(21A)-C(21B)-H(21B2)	111.5 (9)
C(11A)-C(11B)-H(11B3)	103.9 (11)	C(21A)-C(21B)-H(21B3)	101.6 (14)
C(11A)-C(11C)-H(11C1)	109.2 (17)	C(21A)-C(21C)-H(21C1)	128.9 (28)
C(11A)-C(11C)-H(11C2)	112.6 (11)	C(21A)-C(21C)-H(21C2)	107.8 (21)

Table III (*Continued*)

C(11A)–C(11C)–H(11C3)	115.9 (13)	C(21A)–C(21C)–H(21C3)	100.4 (26)
C(12A)–C(12B)–H(12B1)	112.7 (11)	C(22A)–C(22B)–H(22B1)	111.9 (5)
C(12A)–C(12B)–H(12B2)	107.6 (11)	C(22A)–C(22B)–H(22B2)	121.1 (23)
C(12A)–C(12B)–H(12B3)	112.2 (18)	C(22A)–C(22B)–H(22B3)	78.6 (25)
C(12A)–C(12C)–H(12C1)	114.8 (14)	C(22A)–C(22C)–H(22C1)	118.1 (15), 139.7 (31)
C(12A)–C(12C)–H(12C2)	114.0 (12)	C(22A)–C(22C)–H(22C2)	102.0 (17), 105.8 (23)
C(12A)–C(12C)–H(12C3)	103.5 (11)	C(22A)–C(22C)–H(22C3)	113.8 (38), 120.2 (55)
C(13A)–C(13B)–H(13B1)	100.5 (39)	C(23A)–C(23B)–H(23B1)	108.8 (17)
C(13A)–C(13B)–H(13B2)	119.0 (13)	C(23A)–C(23B)–H(23B2)	103.3 (12)
C(13A)–C(13B)–H(13B3)	114.9 (37)	C(23A)–C(23B)–H(23B3)	122.8 (17)
C(13A)–C(13C)–H(13C1)	130.4 (24)	C(23A)–C(23C)–H(23C1)	105.5 (15)
C(13A)–C(13C)–H(13C2)	106.8 (15)	C(23A)–C(23C)–H(23C2)	109.2 (20)
C(13A)–C(13C)–H(13C3	102.8 (17)	C(23A)–C(23C)–H(23C3)	112.6 (17)

[a] Estimated standard deviations are given in parentheses. [b] Atoms of a given type labeled with and without a prime are related to each other by the crystallographic center of inversion. [c] Duplicate distances refer to alternate conformation of one isopropyl group (see Experimental Section).

decided to proceed with data collection.

Lattice constants (Table I) were determined from least-squares fit of 32 reflections ($32° < 2\theta < 58°$). See Table I for details of data collection and structure refinement. A hemisphere of data (4613 reflections) were collected in the θ–2θ step scan mode to a $(\sin\theta)/\lambda$ limit of 0.581 Å^{-1}. During data collection three intense reflections were periodically monitored, and no significant fluctuations were observed.

Data were corrected for absorption with maximum and minimum transmission factors of 0.730 and 0.521, respectively. The value of μ/ρ used for H was 23.9 cm^2/g.[5] Equivalent data were averaged to yield 4224 unique reflections for structure analysis. Scattering lengths used in the analysis are $\bar{b}_{Rh} = 0.58$, $\bar{b}_P = 0.51$, $\bar{b}_O = 0.580$, $\bar{b}_C = 0.665$, and $\bar{b}_H = -0.374$ ($\times 10^{-12}$ cm).

Initially, the Rh, P, O, and C atom positions derived from a room-temperature X-ray analysis were used for structure factor calculation.[3] A difference Fourier synthesis revealed the locations of the hydrogen atoms bridging the Rh–Rh bond and several aliphatic hydrogen atoms. Least-squares refinements followed by difference Fourier syntheses[6] revealed the location of all other hydrogen atoms. At this point the agreement factor was 0.209.[7] Several cycles of least-squares refinement in which the scale factor, positional, and anisotropic thermal parameters were allowed to vary reduced the agreement factor to 0.162. It was then noted that several methyl group hydrogen atoms exhibited large anisotropic thermal ellipsoids and unreasonable C–H distances. The positions of these hydrogen atoms were calculated with assumption of tetrahedral geometry about each carbon atom and a C–H distance of 1.08 Å. It was also noted that one of the isopropyl groups was disordered. In approximately 50% of the molecules, the positions of a methyl group and the corresponding α-hydrogen atom appear exchanged. The remaining methyl group of this isopropyl substituent appeared to occupy similar positions in the two conformations although the large thermal ellipsoids of the hydrogen atoms of this methyl group suggested possible disorder. Examination of the thermal parameters of the other aliphatic hydrogen atoms also suggested disorder, but the limited data set available precluded a resolution of alternative conformations.

Least-squares refinement (in two blocks) was continued, initially fixing the positional parameters of those hydrogen atoms whose positions were calculated and then later allowing all parameters to vary. Convergence was realized at $R_w(F_o^2) = 0.135$. A final difference Fourier synthesis contained numerous small ($<0.2 \times 10^{-12}$ cm/Å^3) negative peaks in regions near methyl group hydrogen atoms. Since none of these peaks were interpretable in terms of alternative conformations of the model, refinement was halted at this point.

An inspection of C–H distances and the thermal parameters of methyl group atoms shows that C–H bond distances that differ appreciably from 1.08 Å coincide with elongated hydrogen atom thermal ellipsoids. This results in large standard deviations for some of the methyl group hydrogen positions. However, the consistency of bond distances and angles in the remainder of the molecule indicates the overall correctness of the structural model and lends confidence to the atomic positions derived from the data. The overall effect of the uncertainty of the methyl group hydrogen atom positions is then merely to lower the precision of the structure analysis.

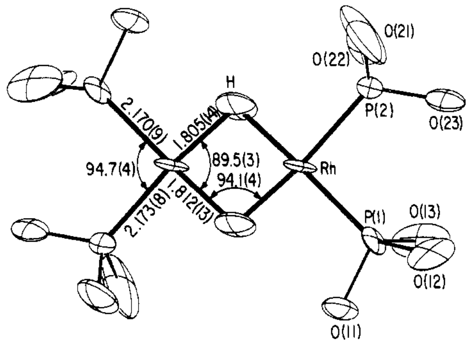

Figure 1. Plot of the inner core of $\{HRh[P(O\text{-}i\text{-}C_3H_7)_3]_2\}_2$ with selected bond distances (Å) and angles (deg). The thermal ellipsoids are drawn to enclose 50% probability. A center of inversion exists midway between the Rh atoms.

Table IV. "Best" Least-Squares Plane through the $P_4Rh_2H_2$ Fragment of $\{HRh[P(O\text{-}i\text{-}C_3H_7)_3]_2\}_2$ with the Equation[a] $0.5565x + 0.4393y - 0.7052z = 0.0$

atom	dist, Å	dist,[b] Å
Rh	0.015 (6)	−0.015 (6)
H	−0.001 (14)	0.001 (14)
P(1)	−0.006 (7)	0.006 (7)
P(2)	−0.001 (8)	0.001 (8)
O(11)[c]	0.091 (7)	−0.091 (7)
C(11A)[c]	0.122 (8)	−0.122 (8)
H(11A)[c]	−0.045 (20)	0.045 (20)
O(23)[c]	−0.215 (7)	0.215 (7)
C(23A)[c]	−0.283 (8)	0.283 (8)
H(23A)[c]	−0.168 (19)	0.168 (19)

[a] The equation of the plane is expressed in the triclinic fractional coordinates x, y, z. [b] Distances from the plane of those atoms related by a center of symmetry. [c] Assigned a weight of zero in the least-squares process.

Results and Discussion

Although the crystal structure of $\{HRh[P(O\text{-}i\text{-}C_3H_7)_3]_2\}_2$ was characterized by a slight disorder (see Table III, footnote *c*) and relatively large-atom thermal motion associated with the methyl groups of the isopropyl substituents, the inner core of this dimer was precisely defined. Final atom positional and thermal parameters are given in Table II, and selected interatomic distances and angles in Table III. A diagram of the inner core of the molecule is presented in Figure 1 and a stereoscopic drawing in Figure 2. Note that a crystallographic center of inversion exists midway between the two Rh atoms.

---

(5) R. G. Teller, R. D. Wilson, R. K. McMullan, T. F. Koetzle, and R. Bau, *J. Am. Chem. Soc.*, **100**, 3071 (1978).

(6) Details of structure refinement and programs used have been reported previously. See J. L. Peterson, L. F. Dahl, and J. M. Williams, *J. Am. Chem. Soc.*, **96**, 6610 (1974). A factor of $(0.03F_o^2)^2$ was added to the variance of each F_o^2.

(7) $R_w(F_o^2) = [\sum w(F_o^2 - F_c^2)^2/\sum wF_o^4]^{1/2}$.

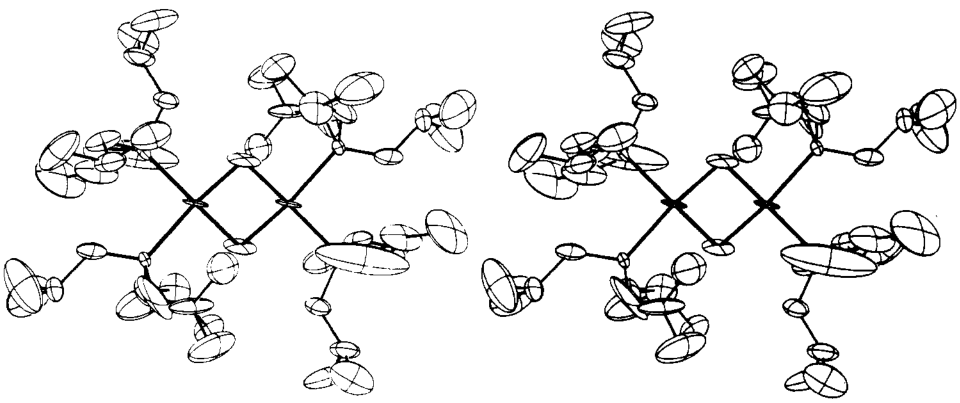

Figure 2. Stereoscopic drawing of $\{HRh[P(O\text{-}i\text{-}C_3H_7)_3]_2\}_2$ with the aliphatic hydrogens omitted for clarity. This view clearly illustrates how the bulky isopropyl phosphite ligands shield the molecule. A close examination of the drawing reveals the noncrystallographic $(C\text{–}O\text{–}P)_2Rh(\mu\text{-}H)_2Rh(P\text{–}O\text{–}C)_2$ mirror plane in the plane of the drawing.

This rhodium dimer, like the analogous trimer $\{HRh[P(OCH_3)_3]_2\}_3$,[2,3,8] is based on square-planar P_2RhH_2 coordination units, but for the dimer there is edge sharing through the two hydride atoms. All of the core nuclei in the dimer, the two hydride hydrogen atoms, the two rhodium atoms, and the four phosphorus atoms are essentially coplanar (Table IV). Despite the disparity in the ligand sizes, the interbond angles are remarkably close to 90°: the P–Rh–P angles are explicably the largest (94.7 (4)°), the H–Rh–H the smallest (85.9 (5)°), and the H–Rh–P average angles very close to 90° (namely, 89.6 (4)°). The Rh_2H_2 unit is a rectangle with Rh–Rh and H–H distances of 2.65 (1) and 2.46 (1) Å. All core interatomic distances are normal and agree well with the results from an earlier X-ray diffraction investigation of the dimer.[3]

The bridging hydrogen atoms in the rhodium dimer do not reside in positions expected from geometric considerations. Both hydrogen atoms are displaced toward the metal–metal bond from the intersection of phosphorous–metal vectors. This may be contrasted with singly hydrogen bridged metal–metal bonds where hydrogen atoms are displaced away from the metal–metal vector with respect to the intersection of phosphorus metal vectors. With a fixed M–M distance, the displacement of the H ligand from the ligating atom–metal atom vector is presumably determined by the M–H bond length.[9] Hence a displacement of the hydrogen atoms away from the M–M bond in $M\text{–}(H)_2\text{–}M$ units would lengthen the M–H bond beyond reasonable values. This relationship appears to be a general observation in $M\text{–}(H)_2\text{–}M$ systems.[10]

The Rh–H distance in this dimer is significantly larger than for $\{HRh[P(OCH_3)_3]_2\}_3$ where there is a single Rh–H–Rh bridge bond: the values are 1.81 (1) and 1.76 (2) Å for the dimer and trimer, respectively.[2,8] These distances may be compared with some bridging M–H distances also determined by neutron diffraction studies: 1.821 (3) Å for Ru–H–Ru in $[HFeRu_3(CO)_{13}^-]$,[11] 1.773 (2) Å for Ru–H–Ru in $H_4Ru_4(CO)_8[P(OCH_3)_3]_4$,[12] 1.792 (5) Å for Ru–H–Ru in $HRu_3(CO)_9(\eta^2\text{-}\mu\text{-}RC_2R)$,[13a] 1.734 (4) Å for Co–H–Co in $HFeCo_3(CO)_9[P(OCH_3)_3]_3$,[13b] and 1.75 (1) Å for Ir–H–Ir in $\{[C_5(CH_3)_5]_2Ir_2H_3^+\}$.[14]

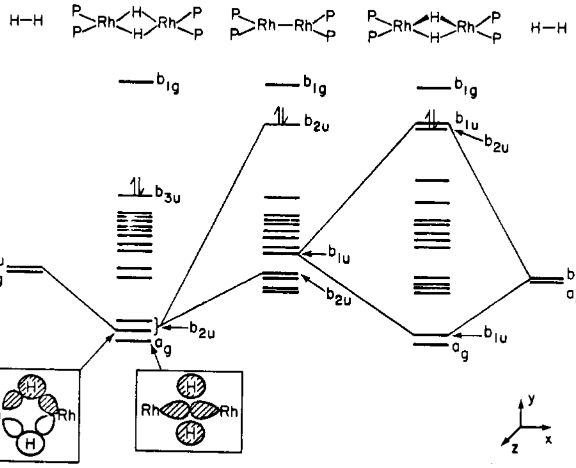

Figure 3. Interaction of a planar Rh_2P_4 fragment with two hydrogen atoms (not to scale). The energy levels for the observed planar $H_2Rh_2P_4$ molecule are shown on the left, while the energy levels for the hypothetical dimer of tetrahedral rhodium atoms are shown on the right. The b_{2u} orbitals shown at left are down in the P(p) and Rh(p) block. See ref 15 for the complete labelling of the molecular orbitals in these three models (drawing not to scale).

The conformation of the phosphite ligands has an exceptional feature. The P–O bonds of each phosphite ligand are either equatorial or axial (approximately parallel or perpendicular, respectively) to the Rh–Rh vector. This generates a planar $(O\text{–}P)_2Rh(\mu\text{-}H)_2Rh(P\text{–}O)_2$ arrangement of axial-equatorial P–O sets at each end of the Rh_2H_2 core. The atomic positions of the C–H atoms of the $CH(CH_3)_2$ fragments of these phosphite ligands are also found in this plane which bisects these $CH_3\text{–}C\text{–}CH_3$ angles and also the O–P–O angle of the remaining isopropoxy groups not associated with this noncrystallographic mirror plane.

An extended Hückel molecular orbital calculation[15] for $\{HRh[P(O\text{-}i\text{-}C_3H_7)_3]_2\}_2$, using the structural parameters established in this study and PH_3 as a model of the phosphite ligand, suggest that the framework bonding is best represented

---

(8) R. K. Brown, J. M. Williams, A. J. Sivak, and E. L. Muetterties, *Inorg. Chem.*, **19**, 370 (1980).

(9) See the discussion on M–H–M bonding in R. Bau, R. G. Teller, S. W. Kirtley, and T. F. Koetzle, *Acc. Chem. Res.*, **12**, 176 (1979).

(10) (a) R. W. Broach and J. M. Williams, *Inorg. Chem.*, **18**, 314 (1979); (b) M. R. Churchill, F. J. Hollander, and J. P. Hutchinson, *ibid.*, **16**, 2697 (1977).

(11) $[(Ph_3P)_2N^+][HFeRu_3(CO)_{13}^-]$: F. Takasagawa, A. Fumagalli, T. F. Koetzle, W. L. Gladfelter, G. L. Geoffrey, M. Bruck, and R. Bau, private communication.

(12) A. G. Orpen, Ph.D. Thesis, Cambridge University, 1979.

(13) (a) $HRu_3(CO)_9[\eta^2\text{-}\mu_3\text{-}C_2(t\text{-}C_4H_9)]$: M. Catti, G. Gervasio, and S. A. Mason, *J. Chem. Soc., Dalton Trans.*, 2260 (1977); (b) R. G. Teller, R. D. Wilson, R. K. McMullan, T. F. Koetzle, and R. Bau, *J. Am. Chem. Soc.*, **100**, 3071 (1978).

(14) $\{[C_5(CH_3)_5]_2Ir_2H_3^+\}[BF_4^-]$: R. Bau, W. E. Carroll, D. W. Hart, R. G. Teller, and T. F. Koetzle, *Adv. Chem. Ser.*, **No. 167**, Chapter 5 (1978).

(15) The program used was obtained from the National Resource for Computational Chemistry, Quantum Chemistry Program Exchange No. 358. The order of the energy levels (increasing energy) was as follows: for the $Rh_2(PH_3)_4$ fragment a_g, b_{1g}, b_{3u}, b_{2u}, b_{1u}, a_g, b_{3g}, a_u, a_g, b_{3u}, b_{2g}, b_{3u}, b_{2u}, b_{1g}; for the planar dimer $H_2Rh_2(PH_3)_4$ a_g, b_{2u}, b_{2u}, b_{3u}, b_{1g}, b_{1u}, a_g, b_{3g}, a_g, a_u, a_g, b_{3u}, b_{2g}, b_{3u}, b_{1g}; for the tetrahedral dimer $H_2Rh_2(PH_3)_4$ a_g, b_{1u}, b_{2u}, a_g, b_{3u}, b_{1g}, a_g, a_u, b_{3g}, b_{3u}, b_{2g}, b_{3u}, a_g, b_{2u}, b_{1u}, b_{1g}.

by two four-center (Rh_2H_2) two-electron bonds, a_g and b_{2u} (Figure 3). The Mulliken bond order for the Rh–Rh interaction was positive but very small (0.086) largely due to Rh p-orbital bonding (0.076) whereas those for the Rh–H bonds were substantial, about 0.5 bond order (0.497), with major contributions from the rhodium s and p orbitals.

A formally related complex is the dimer of the d^9 $\{HNi[(C_6H_{11})_2PC_3H_6P(C_6H_{11})_2]\}_2$ compound, which has a short Ni–Ni bond (2.441 (1) Å) with both hydride ligands symmetrically bridging this bond.[17] The coordination geometry for each nickel atom is not planar but rather is distorted toward a dimer of tetrahedrally coordinated nickel atoms. Specifically, there is a twisting of the P_2Ni planes with respect to the Ni_2H_2 plane, the dihedral angles between the two P_2Ni planes and the Ni_2H_2 plane being ±31.7°. A molecular orbital analysis identified a small barrier for twisting motion in this 30-electron complex, suggesting that the distortion arises from ligand–ligand repulsions. The situation is different for the 28-electron, d^8 $(HRhP_2)_2$ dimer. Distorting the hydride ligands with respect to the Rh_2P_4 framework toward the tetrahedral dimer significantly destabilizes the b_{2u} bonding orbital relative to the b_{3u} HOMO in square-planar $(HRhP_2)_2$ (Figure 3). Hence, in the d^8 $(HRhP_2)_2$ dimer, there is a variation in total energy with a dihedral angle that is large; the tetrahedral dimer extreme is 100.3 kcal/mol higher in energy than the observed square-planar geometry. In contrast, the d^9 $(HNiP_2)_2$ dimer is also stabilized by the b_{1u} metal–metal bonding orbital shown in Figure 3 for the tetrahedral configuration. Thus, distortion is more facile for the d^9 complexes.

Acknowledgment. This collaborative research was supported by the National Science Foundation (Grants CHE-78-20698 and CHE-78-08711). All work at Argonne and Brookhaven National Laboratories was performed under the auspices of the Office of Basic Energy Sciences of the U.S. Department of Energy. The rhodium chloride used in these studies was obtained on a loan grant from Johnson Matthey, Inc. We thank Mr. Joseph Henriques for providing technical assistance during the neutron diffraction experiment.

Registry No. $\{HRh[P(O\text{-}i\text{-}C_3H_7)_3]_2\}_2$, 65176-62-7.

Supplementary Material Available: A listing of the observed and calculated structure factor amplitudes (14 pages). Ordering information is given on any current masthead page.

---

(16) B. L. Barnett, C. Krüger, Y. N. Tsay, R. H. Summerville, and R. Hoffmann, *Chem. Ber.*, **110**, 3900 (1977).

(17) R. H. Summerville and R. Hoffmann, *J. Am. Chem. Soc.*, **98**, 7240 (1976).

Contribution from the Laboratoire de Chimie des Organométalliques, Campus de Beaulieu, Université de Rennes, Rennes, 35042 France, and the Guelph-Waterloo Centre for Graduate Work in Chemistry, Waterloo Campus, University of Waterloo, Waterloo, Ontario, Canada N2L 3G1

Neutral and Cationic (η^2-Dithioalkyl ester)iron(II) Complexes. Synthesis, Spectroscopic Studies, and X-ray Structure of $[Fe(\eta^2\text{-}CS_2CH_2Ph)(CO)_2(PMe_3)_2]PF_6$

DANIEL TOUCHARD,[1a] HUBERT LE BOZEC,[1a] PIERRE H. DIXNEUF,*[1a] ARTHUR J. CARTY,*[1b]
and NICHOLAS J. TAYLOR[1b]

Received August 19, 1980

Reaction of $Fe(\eta^2\text{-}CS_2)(CO)_2L_2$ (**1**) (L = tertiary phosphine or phosphite) with MeI or $PhCH_2Br$ yields cationic complexes $[Fe(\eta^2\text{-}CS_2R)(CO)_2L_2]^+X^-$ (R = Me, $PhCH_2$; X = I, Br) via alkylation at the uncoordinated sulfur atom, of which $[Fe(\eta^2\text{-}CS_2Me)(CO)_2(PPh_3)_2]I$ (**2b**) and $[Fe(\eta^2\text{-}CS_2CH_2Ph)(CO)_2(PPh_3)_2]Br$ (**3b**) have been isolated and characterized in the solid state. The behavior of these cations depends markedly on the nature of L; good donors facilitate CO displacement giving halo complexes $Fe(\eta^2\text{-}CS_2Me)(I)(CO)(PMe_2Ph)_2$ (**6d**), $Fe(\eta^2\text{-}CS_2Me)(I)(CO)(PMe_3)_2$ (**6e**), $Fe(\eta^2\text{-}CS_2CH_2Ph)(Br)(CO)(PMe_2Ph)_2$ (**7d**), and $Fe(\eta^2\text{-}CS_2CH_2Ph)(Br)(CO)(PMe_3)_2$ (**7e**) which are fluxional in solution. Treatment of solutions of the cations $[Fe(\eta^2\text{-}CS_2R)(CO)_2L_2]^+$ with $NaPF_6$ gave excellent yields of $[Fe(\eta^2\text{-}CS_2Me)(CO)_2\{P(OMe)_3\}_2]PF_6$ (**4a**), $[Fe(\eta^2\text{-}CS_2Me)(CO)_2(PPh_3)_2]PF_6$ (**4b**), $[Fe(\eta^2\text{-}CS_2Me)(CO)_2(PMe_2Ph)_2]PF_6$ (**4d**), $[Fe(\eta^2\text{-}CS_2Me)(CO)_2(PMe_3)_2]PF_6$ (**4e**), $[Fe(\eta^2\text{-}CS_2CH_2Ph)(CO)_2(PMe_3)(PPh_3)]PF_6$ (**5c**), $[Fe(\eta^2\text{-}CS_2CH_2Ph)(CO)_2(PMe_2Ph)_2]PF_6$ (**5d**), and $[Fe(\eta^2\text{-}CS_2CH_2Ph)(CO)_2(PMe_3)_2]PF_6$ (**5e**). The complex $[Fe(\eta^2\text{-}CS_2CH_2Ph)(CO)_2(PMe_3)_2]PF_6$ crystallizes in space group $P2_1/n$ with cell dimensions a = 14.403 (2) Å, b = 9.354 (1) Å, c = 18.648 (2) Å, β = 99.56 (1)°, and Z = 4. Refinement based on 3183 observed ($I \geq 3\sigma(I)$) diffractometer data converged at R = 0.036 and R_w = 0.048. The alkylated CS_2 ligand is η^2 coordinated to iron with Fe–C(3) of 1.890 (3) Å, Fe–S(1) of 2.321 (1) Å, and C(3)–S(1) of 1.634 (3) Å. The basic stereochemistry at the iron atom is distorted trigonal bipyramidal with the CS_2CH_2Ph group occupying an equatorial site and the two phosphines in trans positions. Alkylation of the $Fe(\eta^2\text{-}CS_2)$ group leads to a shortening of the Fe–C(CS_2) and coordinated C–S bonds while the uncoordinated C–S bond is lengthened.

Introduction

There is a growing interest in the chemistry of the coordinated CS_2 ligand particularly because derivatives are frequently useful precursors for other interesting transition-metal derivatives. Thus (η^2-dithiomethyl)metal complexes can be converted to thiocarbonyls via alkylthiol elimination,[2] dithiocarbene complexes are accessible from CS_2 complexes via treatment with electrophilic alkynes[3] or excess methyl iodide,[4] metallaheterocycles can be synthesized from acetylenes,[5] and binuclear mixed-metal complexes have been prepared by utilizing the ligating properties of the sulfur atoms.[6,7] More recently, intramolecular fragmentation of CS_2 has led to the

---

(1) (a) Université de Rennes. (b) Guelph-Waterloo Centre.

(2) Collins, T. J.; Roper, W. R.; Town, K. G. *J. Organomet. Chem.* **1976**, *121*, C41.

(3) Le Bozec, H.; Gorgues, A.; Dixneuf, P. H. *J. Am. Chem. Soc.* **1978**, *100*, 3946.

(4) Grundy, K. R.; Harris, R. O.; Roper, W. R. *J. Organomet. Chem.* **1975**, *90*, C34.

(5) Le Bozec, H.; Gorgues, A.; Dixneuf, P. H. *J. Chem. Soc., Chem. Commun.* **1978**, 573.

(6) (a) Werner, H.; Leonhard, K.; Burschka, Ch. *J. Organomet. Chem.* **1978**, *160*, 291. (b) Quick, M. H.; Angelici, R. J. *Ibid.* **1978**, *160*, 231. (c) Fehlhammer, W. P.; Mayr, A.; Stolzenberg, H. *Angew. Chem., Int. Ed. Engl.* **1979**, *91*, 661. (d) Bianchini, C.; Meli, A.; Orlandini, A.; Sacconi, L. *Inorg. Chim. Acta* **1979**, *35*, L375.

(7) Southern, T. G.; Oehmichen, U.; Le Marouille, J. Y.; Le Bozec, H.; Grandjean, D.; Dixneuf, P. H. *Inorg. Chem.* **1980**, *19*, 2976.